Explicit Determination of Robin Parameters in Optimized Schwarz Waveform Relaxation Methods for Schrödinger Equations Based on Pseudodifferential Operators

Xavier Antoine, Emmanuel Lorin

Explicit computation of Robin parameters in Optimized Schwarz Waveform Relaxation methods for Schrödinger equations based on pseudodifferential operators

Xavier Antoine[1,1], Lorin Emmanuel[2]

[1] *Institut Elie Cartan de Lorraine, Université de Lorraine, Sphinx Inria team, Inria Nancy-Grand Est, F-54506 Vandoeuvre-lès-Nancy Cedex, France.*
[2] *School of Mathematics and Statistics, Carleton University, Ottawa, Canada, K1S 5B6. Centre de Recherches Mathématiques, Université de Montréal, Montréal, Canada, H3T 1J4.*

Abstract. The Optimized Schwarz Waveform Relaxation algorithm, a domain decomposition method based on Robin transmission condition, is becoming a popular computational method for solving evolution partial differential equations in parallel. Along with well-posedness, it offers a good balance between convergence rate, computational complexity and simplicity of the implementation. The fundamental question is the selection of the Robin parameter to optimize the convergence of the algorithm. In this paper, we propose an approach to explicitly estimate the Robin parameter which is based on the approximation of the transmission operators at the subdomain interfaces, for the linear/nonlinear Schrödinger equation. Some illustrating numerical experiments are proposed for the one- and two-dimensional problems.

Key words: Optimized Schwarz Waveform Relaxation; domain decomposition method; Schrödinger equation; dynamics; stationary states; Robin boundary condition; pseudodifferential operators; fast convergence.

1 Introduction

Domain decomposition method (DDM) is a general strategy for solving high-dimensional PDEs. Among DDMs, the Schwarz Waveform Relaxation (SWR) method is a popular algorithm for the numerical computation of evolution equations [13–19], in particular wave-like equations. SWR methods are characterized by the choice of the Transmission Conditions (TC) at the subdomain interfaces: Classical SWR is based on Dirichlet TC, Robin SWR uses Robin TC, Optimal SWR is related to transparent TC, and quasi-optimal SWR is based on accurate absorbing TC. Optimized SWR usually refers to Robin SWR, where the Robin parameters are optimized to ensure the fastest convergence possible of the algorithm. The latter then offers a good balance between fast convergence rate and efficient IBVP solver. In this paper, we are specifically interested in Optimized SWR methods. We now briefly describe the Schwarz Waveform Relaxation algorithms and set the problem of the selection of an optimized choice of the Robin parameter in the transmission conditions. Consider a d-dimensional evolution partial differential equation $P\phi = f$ in the spatial domain $\Omega \subseteq \mathbb{R}^d$, and time domain (t_1,t_2), where $t_2 > t_1 \geqslant 0$. The initial data is denoted by ϕ_0. We first split Ω into two open subdomains

[1]Corresponding author. *Email addresses:* xavier.antoine@univ-lorraine.fr (X. Antoine), elorin@math.carleton.ca (E. Lorin)

$\Omega_\varepsilon^\pm$ with smooth boundary, with or without overlap ($\overline{\Omega}_\varepsilon^+ \cap \overline{\Omega}_\varepsilon^- = \emptyset$ or $\Omega_\varepsilon^+ \cap \Omega_\varepsilon^- \neq \emptyset$), with $\varepsilon > 0$. The SWR algorithm consists in iteratively solving IBVPs in $\Omega_\varepsilon^\pm \times (t_1, t_2)$, using transmission conditions at the subdomain interfaces $\Gamma_\varepsilon^\pm := \partial\Omega_\varepsilon^\pm \cap \Omega_\varepsilon^\mp$, where the imposed conditions are established using the preceding Schwarz iteration data in the adjacent subdomain. The Robin-Schwarz Waveform Relaxation algorithm can be seen as an approximate version of Optimal SWR algorithm [7], where the transparent transmission operator is approximated by a Robin transmission operator as follows, see also [1,21]: for $k \geqslant 1$, and denoting $\phi^\pm$ the solution in $\Omega_\varepsilon^\pm$ we define

$$\left\{ \begin{array}{lcl} P\phi^{\pm,(k)} & = & f, \text{ in } \Omega_\varepsilon^\pm \times (t_1, t_2), \\ \phi^{\pm,(k)}(\cdot, 0) & = & \phi_0^\pm, \text{ in } \Omega_\varepsilon^\pm, \\ \mathcal{T}_\pm \phi^{\pm,(k)} & = & \mathcal{T}_\pm \phi^{\mp,(k-1)}, \text{ on } \Gamma_\varepsilon^\pm \times (t_1, t_2), \end{array} \right. \tag{1.1}$$

with a given initial guess $\phi^{\pm,(0)}$, and $\mathcal{T}^\pm = \nabla_{\boldsymbol{n}^\pm} \pm \mathtt{i}\lambda_{\Gamma_\varepsilon}^\pm$ with $\lambda_{\Gamma_\varepsilon^\pm}^\pm \in \mathbb{R}^*$ or $\mathtt{i}\mathbb{R}^*$, and outward normal vector $\boldsymbol{n}^\pm$ to $\Gamma_\varepsilon^\pm$.

Our strategy to select the Robin parameter is based on existing results on the convergence rate of SWR methods. As it is well-known [6, 7, 14], for quantum wave equations the fastest convergence rate of SWR methods is obtained with transparent transmission conditions leading to the so-called Optimal SWR method. The latter is however usually very inefficient due to their computational complexity [7]. In order to select the Robin parameter, we then first i) approximate the symbol of the transparent transmission operator in the asymptotic regime, ii) reconstruct the corresponding operator at the interface.
Although, the general idea is in principle applicable to a large class of PDE, we will focus in this paper on the Schrödinger equation i) in real-time and ii) imaginary-time within the Normalized Gradient Flow method (NGF) for computing the Schrödinger Hamiltonian point spectrum [6,7,10]. In the first work on OSWR for the one-dimensional Schrödinger equation [14,20], the authors assume that the transmission conditions are of Robin type, and then optimize the constant to get the fastest convergence from a convergence rate established for a fixed-point contraction factor. In our work, the approach is different : we actually first construct the transparent operator at the subdomain interfaces, then locally approximate this operator. Let us also cite, some recent works by Besse and Xing [9, 11, 12], where the transparent operator is approximated by using Padé approximants or Taylor's expansions.

The paper is organized as follows. In Section 2, we present the detailed approach for selecting the Robin parameter in one dimension for the Schrödinger equation, in real- and imaginary-time. Some numerical experiments are then proposed to illustrate the different ideas exposed in this section. We extend the method along with numerical experiments in higher dimension in Section 3. We finally conclude in Section 4.

2 Optimized parameter in Robin-Schwarz Waveform Relaxation algorithm: one-dimensional case

2.1 Selection of the Robin parameter

In this paper, we study the question on how to optimize the Robin parameter to fasten the convergence rate and how to choose the interface locations in Schwarz waveform relaxation domain decomposition methods. It was established in [7] that the convergence rate for the SWR method is in particular depending on the location of the subdomain interfaces with respect to the external potential; the interfaces should be located close to local maxima (resp. minima) of positive (resp. negative) potentials. The location of the interfaces is then governed

by a balance between workload on each subdomain, and potential local maxima, as the convergence rate is basically determined by the least local contraction factor [7]. The approach we propose is then slightly different from the one proposed in [20], where the optimization of the parameter is obtained *a posteriori*, assuming the transmission conditions of Robin type. The most common SWR method used in the literature is the optimized SWR method, where the transmission condition is provided by a Robin operator $\mathcal{T}=\partial_x\pm \mathtt{i}\lambda$ (in 1-d), where λ is an optimized Robin parameter. This will provide a well-balanced choice between relatively fast convergence, computational complexity and well-conditioned linear systems. The approach that we propose is as follows. It is proven that the best convergence rate is obtained with transparent transmission conditions, that is using the operator $\partial_x+\mathtt{i}\Lambda^{\pm}(t,x)$, where $\Lambda^{\pm}$ is a transparent pseudodifferential operator involved in the Nirenberg factorization of the main operator P at the subdomain interfaces, which is a second-order operator in space and first-order in time, and such that

$$P(t,x,\partial_t,\partial_x)=(\partial_x+\mathtt{i}\Lambda^-)(\partial_x+\mathtt{i}\Lambda^+)+\mathcal{R}, \tag{2.1}$$

where $\mathcal{R}\in \mathrm{OPS}^{-\infty}$. In general, $\partial_x+\mathtt{i}\Lambda^{\pm}$ is a non-local (Dirichlet-to-Neumann) operator, making the so-called Optimal SWR methods inefficient from a computational point of view. A natural approach then consists in approximating the operator symbol $\lambda^{\pm}(\tau,x)=\sigma(\Lambda^{\pm}(\partial_t,x))$ by a constant, setting τ as the co-variable to t. The approach that we propose here is based on an *a priori* optimization of the parameter λ. We can formally construct $\lambda^{\pm}$ as a symbolic asymptotic expansion [3] following

$$\lambda^{\pm}\sim\sum_{j=0}^{+\infty}\lambda^{\pm}_{1/2-j/2},\qquad (\text{ or } \lambda^{\pm}\sim\sum_{j=0}^{+\infty}\lambda^{\pm}_{1-j} \text{ for order-2 in time } P). \tag{2.2}$$

The truncation at order p of the series defining $\lambda^{\pm}$ provides the following estimates for large values of the frequency $|\tau|$

$$\lambda^{+}(\pm\varepsilon/2,\tau)-\lambda^{+,p}(\pm\varepsilon/2,\tau)=\sum_{j=p+1}^{+\infty}\lambda^{+}_{1/2-j/2}(\pm\varepsilon/2,\tau)=\mathcal{O}\big(\frac{1}{(\lambda^{+}_{1/2}(\pm\varepsilon/2,\tau))^{p}}\big). \tag{2.3}$$

For the Schrödinger equation with $P=\mathtt{i}\partial_t+\partial_{xx}-V(x)$, let us recall that [7]

$$\lambda^{\pm}_{1/2}(\tau,x)=\mp\sqrt{-\tau-V(x)}. \tag{2.4}$$

The next symbols are given by

$$\lambda^{\pm}_{0}(\tau,x)=0,\quad \lambda^{\pm}_{-1/2}(\tau,x)=0\quad\text{and}\quad \lambda^{\pm}_{-1}(\tau,x)=\pm\frac{\mathtt{i}}{4}\frac{\partial_x V(x)}{-\tau-V(x)}. \tag{2.5}$$

This leads to the following proposition.

Proposition 2.1. For ξ_i belonging to an interface $\Gamma^{\pm}_{\varepsilon}$, we approximate $\Lambda^{\pm}(\xi_i,\partial_t)$ by a constant $\lambda^{\pm}_{\xi_i}$ as follows: at the discrete level in time, we choose $|\tau_{\text{num.}}|:=1/\Delta t$ (Δt is the time step), for any $p\in\mathbb{N}$, and we fix

$$\lambda^{\pm}_{\xi_i}=\lambda^{\pm}(\xi_i,\tau_{\text{num.}})=\pm\sum_{j=0}^{p}\lambda^{+}_{1/2-j/2}(\xi_i,\tau_{\text{num.}}).$$

In practice, we can take $p\leqslant 1$, in real-time, we then select:

$$\lambda^{\pm}_{\xi_i}=\lambda^{\pm}(\xi_i,\tau_{\text{num.}})=\mp\sqrt{-\tau_{\text{num.}}+V(\xi_i)}. \tag{2.6}$$

In imaginary-time, we replace τ by $-\mathtt{i}\tau$, and consider

$$\lambda^{\pm}_{\xi_i} = \lambda^{\pm}(\xi_i, \tau_{\text{num.}}) = \mp e^{\mathtt{i}\pi/4}\sqrt{-\tau_{\text{num.}} + \mathtt{i}V(\xi_i)}. \tag{2.7}$$

This choice of $\lambda^{\pm}_{\xi_i}$ gives a reasonable approximation of the exact transparent operator at the interfaces in the asymptotic regime, thus providing a fast convergence of the OSWR algorithm. In the nonlinear case $P = \mathtt{i}\partial_t + \partial_{xx} - V(x) - \kappa|\phi|^2$, we have conjectured that a similar estimate holds in the asymptotic regime as the solution is close to an (time-independent) eigenstate. We then propose:

Proposition 2.2. At t_n fixed and for $\phi(\cdot, t_n)$ close enough to an eigenstate, the Robin parameter in OSWR algorithm for $P = \mathtt{i}\partial_t + \partial_{xx} - V(x) - \kappa|\phi|^2$ in imaginary-time is fixed by

$$\lambda^{\pm}_{\xi_i} = \lambda^{\pm}(\xi_i, \tau_{\text{num.}}, t_n) = \mp e^{\mathtt{i}\pi/4}\sqrt{-\tau_{\text{num.}} + \mathtt{i}(V(\xi_i) + \kappa|\phi(\xi_i, t_n)|^2)}.$$

In fact, it is usually not necessary to include the nonlinearity in the choice of the Robin parameter, whenever $\varepsilon > 0$. Indeed, it was conjectured [7] that the convergence rate of SWR method in the nonlinear case is of the form [7]:

$$\begin{aligned} L_\varepsilon(\tau) \approx \Big| \left(\frac{\tau - \mathtt{i}V(-\varepsilon/2) - \mathtt{i}\kappa|\phi_s(-\varepsilon/2)|^2}{\tau - \mathtt{i}V(+\varepsilon/2) - \mathtt{i}\kappa|\phi_s(\varepsilon/2)|^2} \right)^{1/2} \Big| / |\tau|^p \\ \times \Big| \exp\big(-2e^{-\mathtt{i}\pi/4} \int_{-\varepsilon/2}^{\varepsilon/2} \sqrt{-\tau + \mathtt{i}V(y) + \mathtt{i}\kappa|\phi_s(y)|^2} dy \big) \Big|, \end{aligned}$$

or for large $|\tau|$, as

$$L_\varepsilon(\tau) \approx \exp\Big(-\varepsilon\sqrt{2|\tau|} - \frac{1}{\sqrt{2|\tau|}} \int_{-\varepsilon/2}^{\varepsilon/2} V(y) + \kappa|\phi_s(y)|^2 dy \Big) / |\tau|^p,$$

with $p \in \mathbb{N}^*$ and where ϕ_s is an eigenstate. In other words for $\varepsilon > 0$, the convergence rate is mainly ensured by the exponential term (still present in the CSWR method) if $\kappa|\phi_s(\pm\varepsilon/2)|^2$ is large. If the latter is small then the effect of the nonlinearity in the Robin parameter, will anyway not have a strong impact on the convergence for large $|\tau|$. If $\varepsilon = 0$, i.e. without overlap, the contribution of the nonlinearity in the Robin parameter could however be non-negligible.

Let us remark that an "optimized" value of the Robin parameter is intend to provide a largest slope in the asymptotic regime, compared to other Robin parameters, but does not necessarily ensure an overall faster convergence, as the above results are only valid in the asymptotic regime, meaning here for $|\tau|$ large.

2.2 Arbitrary number of subdomains

We now discuss the case of a decomposition with an arbitrary number of subdomains $m \geqslant 2$. We propose the following decomposition (with possible overlap): $\Omega = \cup_{i=1}^m \Omega_i$, such that $\Omega_i = (\xi_i^-, \xi_i^+)$, for $2 \leqslant i \leqslant m-1$, $\Omega_1 = (-a, \xi_1^+)$ and $\Omega_m = (\xi_m^-, +a)$ (see Fig. 1).

Moreover, the overlapping size is: $\xi_i^+ - \xi_{i+1}^- = \varepsilon > 0$, and $|\Omega_i| = L + \varepsilon$, where L is assumed to be much larger than ε. We denote by $\phi_i^{(k)}$, the solution in Ω_i at Schwarz iteration k. We also have $\xi_{i+1}^{\pm} - \xi_i^{\pm} = L$. We consider the following systems

$$\begin{cases} P(x, \partial_t, \partial_x)\phi_i^{(k)} = 0, \quad x \in \Omega_i, \\ \phi_i^{(k)}(0, \cdot) = \varphi_0, \quad x \in \Omega_i, \\ \big(\partial_x + \mathtt{i}\lambda^+_{\xi_i^+}\big)\phi_i^{(k)}(t, \xi_i^+) = \big(\partial_x + \mathtt{i}\lambda^+_{\xi_i^+}\big)\phi_{i+1}^{(k-1)}(t, \xi_i^+), \\ \big(\partial_x + \mathtt{i}\lambda^-_{\xi_i^-}\big)\phi_i^{(k)}(t, \xi_i^-) = \big(\partial_x + \mathtt{i}\lambda^-_{\xi_i^-}\big)\phi_{i-1}^{(k-1)}(t, \xi_i^-). \end{cases} \tag{2.8}$$

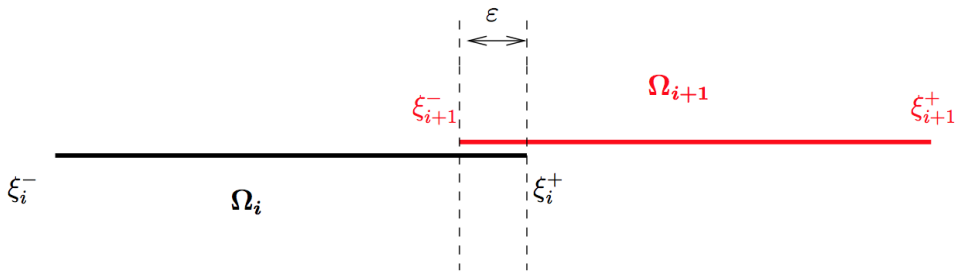

Figure 1: Domain decomposition with possible overlapping.

We have denoted by $P(x,\partial_t,\partial_x)$ the Schrödinger operator in real- or imaginary-time, while $\lambda_{\xi_i}^+$ is the Robin parameter at ξ_i^+ and $\lambda_{\xi_j}^-$ at ξ_{i+1}^-, where $\xi_i^+ - \xi_{i+1}^- = \varepsilon$. We then select the Robin coefficients according to (2.7) (resp. (2.6)) in imaginary- (resp. real-) time. We refer to [8] for details about the convergence of SWR methods with an arbitrary number of subdomains. The selection of the Robin parameters $\lambda_{\xi_i^\pm}^\pm$ is based on the exact same strategy as in Proposition 2.1.

2.3 Numerical experiments

In the one-dimensional case and for $a>0$, we introduce $\Omega_a=(-a,+a)$, $\Omega_{a,\varepsilon}^+=(-a,\varepsilon/2)$ and $\Omega_{a,\varepsilon}^-=(-\varepsilon/2,+a)$, where ε is a (small compared to a) parameter equal to the size of the overlapping region. Null Dirichlet boundary conditions are imposed at $\pm a$. In the following tests, the domains overlap on o nodes. The spatial mesh size Δx is assumed to be constant and then $\varepsilon=(o-1)\Delta x$, which is the length of the overlapping zone. Simple time/space finite difference approximations are proposed to illustrate the methodology presented in this paper. Let us note that the above strategy is independent of the spatial discretization of the equation.

At a given level and in real-time, we consider the following Crank-Nicolson scheme [4]. Denoting by $\phi^{\pm,n,(k)}$ the approximate solution in $\Omega^\pm$ at time t_n with $n\geqslant 0$ and at Schwarz iteration $k\geqslant 0$, the Robin-SWR algorithm reads

$$\left\{\begin{array}{rcl} \mathtt{i}\dfrac{\phi^{\pm,n+1,(k)}-\phi^{\pm,n,(k)}}{\Delta t} & = & -\partial_x^2\dfrac{\phi^{\pm,n+1,(k)}+\phi^{\pm,n,(k)}}{2}+V(x)\dfrac{\phi^{\pm,n+1,(k)}+\phi^{\pm,n,(k)}}{2} \\ & & +\kappa|\phi^{\pm,n+1,(k)}+\phi^{\pm,n,(k)}|^2\dfrac{\phi^{\pm,n+1,(k)}+\phi^{\pm,n,(k)}}{8}=0, \text{ in } \Omega_{a,\varepsilon}^\pm, \\ \left(\partial_{\mathbf{n}^\pm}+\mathtt{i}\lambda_{\pm\varepsilon/2}^\pm\right)\phi_{\pm,\varepsilon/2}^{n+1,(k)} & = & \left(\partial_{\mathbf{n}^\pm}+\mathtt{i}\lambda_{\pm\varepsilon/2}^\pm\right)\phi_{\varepsilon/2}^{\mp,n+1,(k-1)}, \text{ on } \{\pm\varepsilon/2\}. \end{array}\right. \tag{2.9}$$

for the given parameters $\lambda_{\pm\varepsilon/2}^\pm\in\mathbb{R}^*$ and where n denotes the time index. The SWR convergence rate is defined as the slope of the logarithm of the residual history according to the Schwarz iteration number, that is $\{(k,\log(\mathcal{E}^{(k)})):k\in\mathbb{N}\}$, with (for 2 subdomains)

$$\mathcal{E}^{(k)}:=\sum_{i=1}^{2}\Big\| \|\phi_i^{(k)}\big|_{(\xi_{i+1}^-,\xi_i^+)}-\phi_{i+1}^{(k)}\big|_{(\xi_{i+1}^-,\xi_i^+)}\|_\infty\Big\|_{L^2(0,T)}\leqslant\delta^{\mathrm{Sc}}, \tag{2.10}$$

δ^{Sc} being a small parameter.

In imaginary-time, we replace Δt by $\mathtt{i}\Delta t$ in (2.9), and we normalize the solution at each time iteration, i.e.

$$\phi^{\pm,n+1,(k)} \leftarrow \frac{\phi^{\pm,n+1,(k)}}{\|\phi^{n+1,(k)}\|_{L^2(\Omega_a)}},$$

where $\phi^{n+1,(k)}$ denotes the reconstructed solution in Ω_a, at time iteration $n+1$ and Schwarz iteration k, and with $\lambda \in \mathtt{i}\mathbb{R}^*$. The NGF convergence criterion is given by

$$\|\phi^{\pm,(k)}(\cdot,t_{n+1}) - \phi^{\pm,(k)}(\cdot,t_n)\|_{L^\infty(\Omega_a)} \leqslant \delta, \tag{2.11}$$

for some $\delta > 0$ small enough. The SWR convergence rate is defined as the slope of the logarithm of the residual history with respect to the Schwarz iteration number, i.e. $\{(k,\log(E^{(k)})) : k \in \mathbb{N}\}$, where (for 2 subdomains)

$$E^{(k)} := \sum_{i=1}^{2} \Big\| \ \|\phi_i^{\mathrm{cvg},(k)}\big|_{(\xi_{i+1}^-,\xi_i^+)} - \phi_{i+1}^{\mathrm{cvg},(k)}\big|_{(\xi_{i+1}^-,\xi_i^+)}\|_\infty \Big\|_{L^2(0,T^{(k^{\mathrm{cvg}})})} \leqslant \delta^{\mathrm{Sc}}, \tag{2.12}$$

and $\phi_i^{\mathrm{cvg},(k)}$ (resp. $T^{(k^{\mathrm{cvg}})}$) denotes the NGF converged solution (resp. time) in Ω_i at Schwarz iteration k, δ^{Sc} being a small parameter. More details can be found in [7].

Test 1. We first consider the Schrödinger equation in real-time. We introduce $\Omega_{a,\varepsilon}^+ = (-a, 5/2 + \varepsilon/2)$ and $\Omega_{a,\varepsilon}^- = (5/2 - \varepsilon/2, +a)$, with $\varepsilon > 0$ and $a = 10$. Homogeneous Dirichlet boundary conditions are imposed at $\pm a$. The final real-time is set to $T = 0.5$. In the equation, we choose $V(x) = -50\exp(-x^2)$. In addition, the initial data is given by a Gaussian profile

$$\phi_0(x) = \exp\Big(-\frac{1}{5}\big(\frac{b+2a}{4} - x\big)^2\Big)\exp(2\mathtt{i}x).$$

In this first test-case, the numerical data are as follows: $N = 400$, and the overlapping region covers 2 nodes, that is $\varepsilon = \Delta x$. The time step is fixed to $\Delta t = 2 \times 10^{-2}$. Initially, we take $\phi^{(0)}$ as the null function. We report in Fig. 2, the amplitude of the initial data and of the converged solution and the interface location (Left), as well as a comparison of the convergence rate as a function of the Schwarz iteration for different values of the Robin parameter (Right). This result illustrates that defining λ according to the approximate symbol allows for an optimized convergence of the Robin-SWR algorithm in real-time.

Test 2. We next consider the Schrödinger equation in imaginary-time, the following potential $V(x) = 10x^2 + 25\cos^2(\pi x/2)$. The initial data is given by $\phi_0(x) = x\exp(-x^2/2)\pi^{-1/4}$. The two subdomains are $\Omega_{a,\varepsilon}^+ = (-a, \varepsilon/2)$ and $\Omega_{a,\varepsilon}^- = (-\varepsilon/2, +a)$, with $a = 5$. We take $N = 128$ corresponding to $\Delta x = 5/64$. The overlapping region still covers two nodes ($o = 2$): $\varepsilon = (o-1)\Delta x$. The time step is equal to $\Delta t = 2 \times 10^{-2}$. The convergence parameter in (2.11) for the NGF is fixed to $\delta = 10^{-9}$. We show in Fig. 3, the converged solution, and a comparison between different values of the Robin parameters including the "optimized" one showing the largest slope.

We next add a quadratic nonlinearity of strength $\kappa = 50$. We select the following initial data $\phi_0(x) = \exp(-x^2/2)\pi^{-1/4}$ (resp. $\phi_0(x) = x\exp(-x^2/2)\pi^{-1/4}$). The results are plotted in Fig. 4 (resp. Fig. 5) corresponding to the groundstate (resp. first excited state). Although the slope of the residual history in the asymptotic regime is larger for the "optimized" value of the Robin parameters, it does not provide the fastest convergence (in term of number of Schwarz iterations).

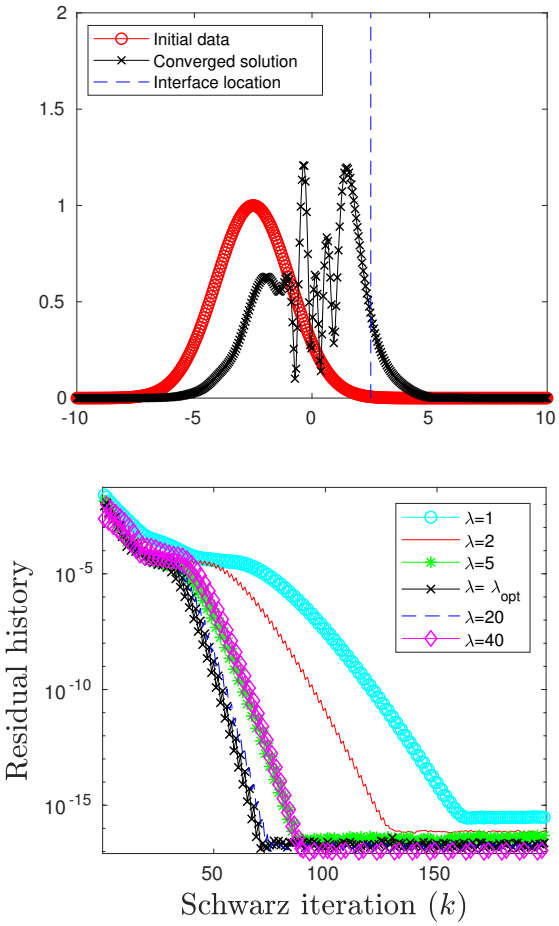

Figure 2: (Left) Amplitude of the initial data and of the converged solution with location of the interface. (Right) Comparison of the SWR convergence rate as a function of the Schwarz iterations with different values of λ.

Test 3. We now analyze the convergence of Robin-SWR on multi-subdomains, in imaginary-time. The Robin parameter is evaluated at the interfaces by using (2.7). We consider the same decomposition as proposed in Subsection 2.2 on $\Omega = (-5,5)$, which is decomposed into $m = 8$ subdomains, with $\Omega_i^+ = (\xi_i^-, \xi_i^+)$ of length $L = 5/4$. In the equation, we choose $V(x) = 5x^2 + 25\cos^2(\pi x/2)$, and the initial data is given by $\phi_0(x) = x\exp(-x^2/2)$. The numerical data are as follows: $N = 512$, and the overlapping regions cover 2 nodes, that is $\varepsilon = \Delta x$. The time step is fixed to $\Delta t = 10^{-1}$. Initially, we take $\phi^{(0)}$ as the null function. They are 8 subdomains, then 7 pairs of Robin parameters to evaluate at each interface, and denoted by $(\lambda_{\xi_i}^+, \lambda_{\xi_i}^-)$ at (ξ_i^+, ξ_{i+1}^-). We compare the convergence rate with the optimal values computed in (2.7) to *randomly* chosen values $\lambda_{\xi_i}^{\pm} \in (0,20)$ at each interface ξ_i^+ and ξ_{i+1}^-. We report in Fig. 6 the amplitude of the initial data and of the converged solution and the interface location (Left), as well as a comparison of the convergence rate vs. the Schwarz iteration for 6 different sets of values of the Robin parameters (Right). This result illustrates that defining λ according to the approximate symbol allows for an optimized convergence of the Robin-SWR algorithm.

Test 4. In this test, we compare the rate of convergence for different values of the optimized Robin parameter in the nonlinear case and in imaginary-time. More specifically, we are going to compare the rate of convergence, when we select

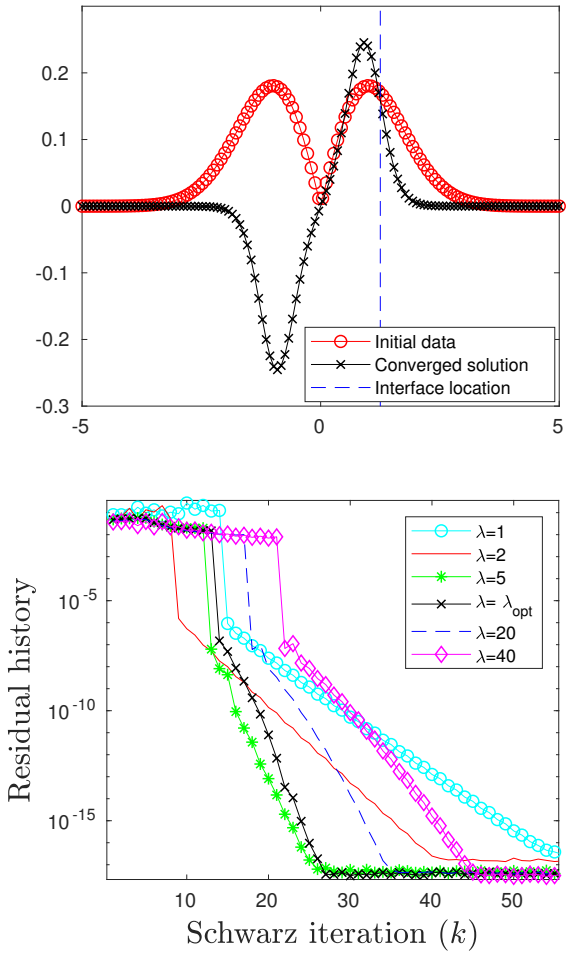

Figure 3: (Left) Modulus the initial data and of the converged eigenstate with location of the interface. (Right) Comparison of the SWR convergence rate as a function of the Schwarz iterations with different values of λ.

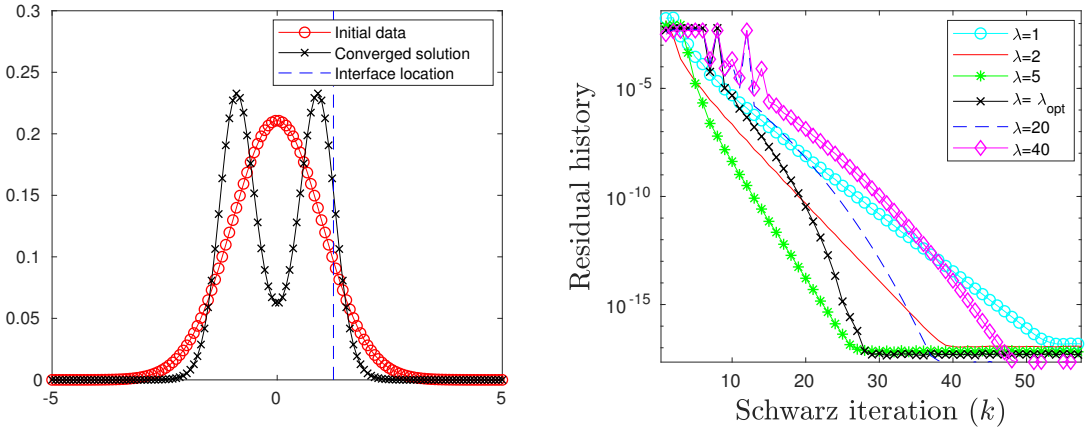

Figure 4: (Left) Amplitude of the initial data and of the converged eigenstate with location of the interface. (Right) Comparison of the SWR convergence rate as a function of the Schwarz iterations with different values of λ.

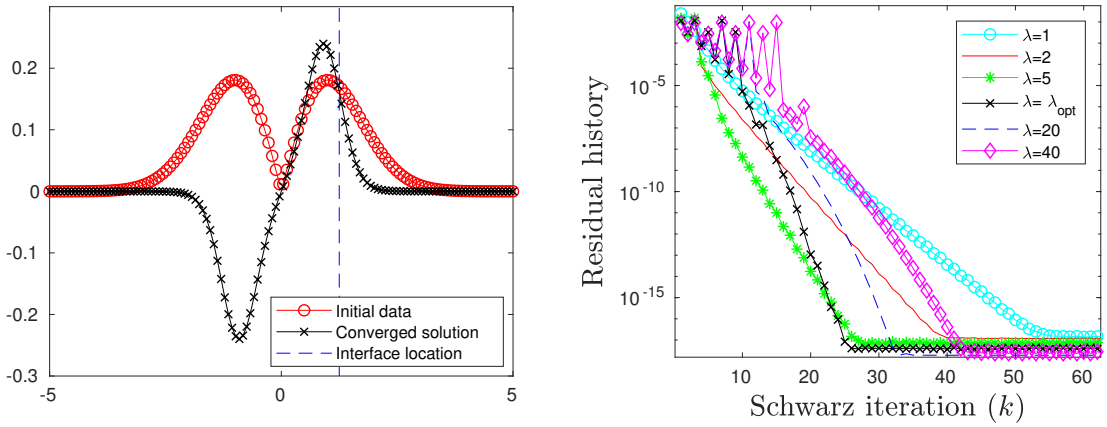

Figure 5: (Left) Amplitude of the initial data and of the converged first eigenstate with location of the interface. (Right) Comparison of the SWR convergence rate as a function of the Schwarz iterations with different values of λ.

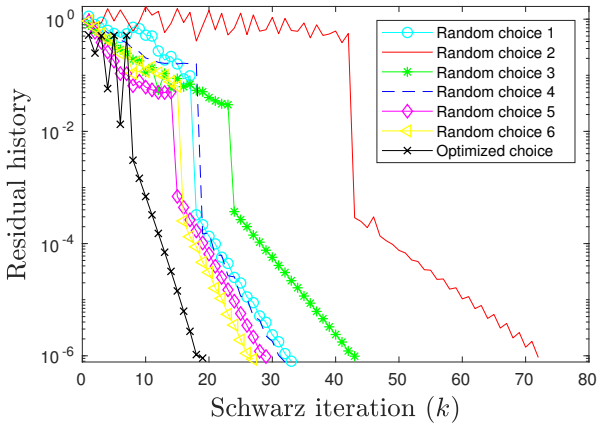

Figure 6: Comparison of the SWR convergence rate as a function of the Schwarz iterations with different values of $\lambda_i^{\pm}$ on 8 subdomains.

- $\lambda^{\pm}_{\text{Opt.1}} = \mp e^{\mathrm{i}\pi/4}\sqrt{-\tau_{\text{num.}}}$,
- $\lambda^{\pm}_{\text{Opt.2}} = \mp e^{\mathrm{i}\pi/4}\sqrt{-\tau_{\text{num.}} + \mathrm{i}V(\xi)}$,
- $\lambda^{\pm}_{\text{Opt.3}} = \mp e^{\mathrm{i}\pi/4}\sqrt{-\tau_{\text{num.}} + \mathrm{i}\left(V(\xi) + \kappa|\phi(\xi,t_n)|^2\right)}$,

with $\xi = 1.25$ with $|\tau_{\text{num.}}| = 1/\Delta t$. We expect that the third choice $\lambda^{\pm}_{\text{Opt.3}}$ would give the best convergence rate, as long as the linear potential and the converged eigenstate are non-null at the interface. Indeed, this last choice corresponds to the best approximation of the transparent operator symbol in the asymptotic regime (where the numerical solution is close to a (time-independent) eigenstate). We consider a nonlinear equation with linear potential $V(x) = 5(x-1/4)^2 + 20\cos^2(\pi x/2)$ and a nonlinearity of strength $\kappa = 100$. The two subdomains are $\Omega^+_{a,\varepsilon} = (-a, \varepsilon/2)$ and $\Omega^-_{a,\varepsilon} = (-\varepsilon/2, +a)$, with $a = 5$. We take $N = 128$ corresponding to $\Delta x = 5/128$. The overlapping region covers two nodes ($o = 2$): $\varepsilon = (o-1)\Delta x$. The time step is equal to $\Delta t = 10^{-2}$. The convergence parameter in (2.11) for the NGF is fixed to $\delta = 10^{-9}$. We select the following initial data $\phi_0(x) = \exp(-x^2/2)\pi^{-1/4}$. We report in Fig. 7, the residual

history for the 3 different values of the optimized Robin parameter. A zoom of the residual history in the asymptotic zone shows in Fig. 8 (Left) that the effect of the nonlinearity in the Robin parameter is negligible for the reasons explained in Section 2 and recalled below. The corresponding groundstate is represented in Fig. 8 (Right). The results are consistent with the analysis of convergence of SWR methods: the fact that the ground state in non-zero at the interface, theoretically makes $\lambda^{\pm}_{\text{Opt.3}}$ more relevant than $\lambda^{\pm}_{\text{Opt.2}}$. However, at the interface the nonlinear term is very small compared to the linear potential and the dominant frequency term, which explains that there is a negligible difference between the results obtained with $\lambda^{\pm}_{\text{Opt.2}}$ and $\lambda^{\pm}_{\text{Opt.3}}$.

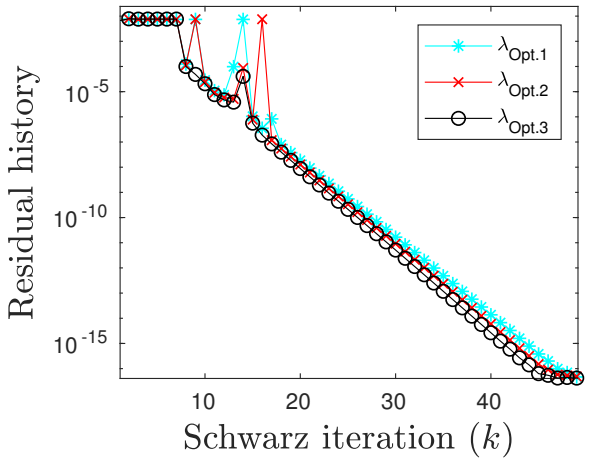

Figure 7: Comparison of the SWR convergence rate as a function of the Schwarz iterations with different values of optimized λ.

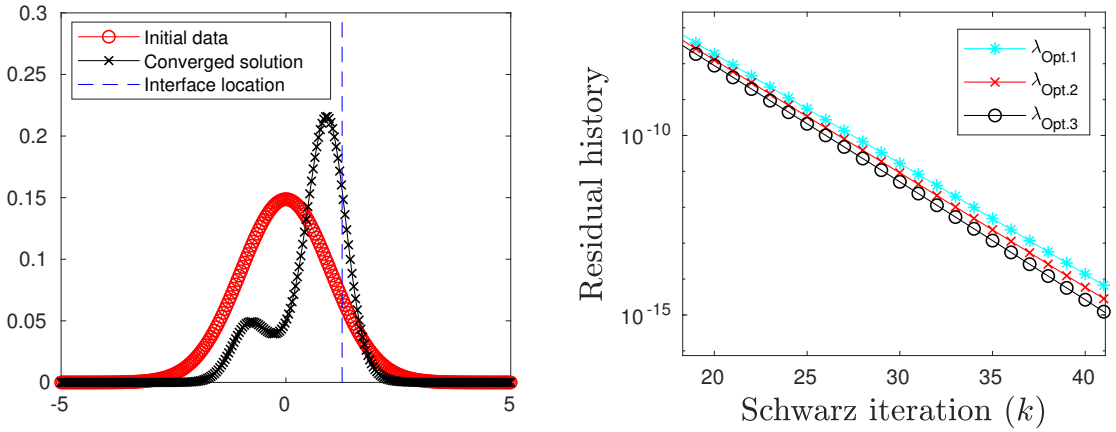

Figure 8: (Left) Amplitude of the initial data and of the converged groundstate with location of the interface. (Right) Zoom in the asymptotic region with different values of optimized λ.

Test 5. In this last one-dimensional test, we compare the rate of convergence of the OSWR method in imaginary-time with $\lambda^{\pm}_{\text{Opt.}} = \mp e^{\mathrm{i}\pi/4}\sqrt{-\tau_{\text{num.}} + \mathrm{i}V(\xi)}$, where the interface is respectively located at $\xi = 0$ and $\xi = 1$. We consider a nonlinear equation with a quartic potential plus an optical lattice : $V(x) = 10(x-1)^2(x+1)^2 + 5\cos^2(\pi x/2)$ and a nonlinearity of strength $\kappa = 200$. The two subdomains are $\Omega^{+}_{a,\varepsilon} = (-a, \varepsilon/2)$ and $\Omega^{-}_{a,\varepsilon} = (-\varepsilon/2, +a)$, with $a = 2$. We take $N = 128$ cor-

responding to $\Delta x = 5/128$. The overlapping region covers two nodes ($o = 2$): $\varepsilon = (o-1)\Delta x$. The time step is equal to $\Delta t = 10^{-2}$. We select the following initial data $\phi_0(x) = \exp(-x^2/2)\pi^{-1/4}$. We report in Fig. 9 the residual history for the 2 different interface locations. As expected, the convergence is faster at the interface $\xi = 0$ compared to $\xi = 1$ since $V(0) > V(1)$. This illustrates the importance of properly locating the subdomain interfaces as function of the linear/nonlinear potential extrema.

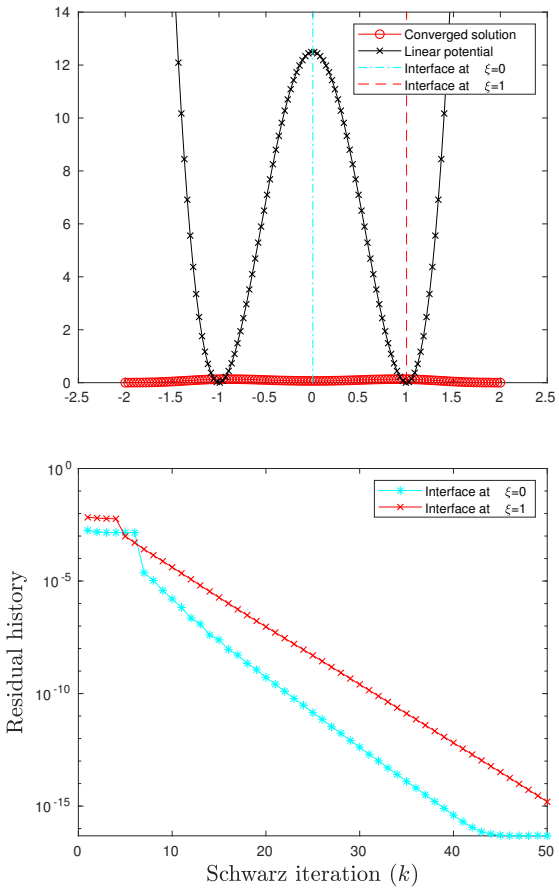

Figure 9: (Left) Linear potential and 2 interface locations. (Right) Comparison of the SWR convergence rate for 2 interface locations.

3 Optimized parameter in Robin-Schwarz Waveform Relaxation algorithm: multi-dimensional case

In this section, we generalize in two-dimensions the ideas developed in Section 2. Basically, the principle is still the approximation by a constant of the operator $\Lambda^{\pm}$ at the subdomain interfaces, where the latter is obtained by a preliminary construction of transparent operators, thanks to a Nirenberg factorization of the operator under consideration. Unlike the one-dimensional case, this naturally requires non-trivial analytical work, which is now detailed. Additional informations can also be found in [6]. Extending the method to a general dimension d is more complicate but possible. It requires some advanced differential geometry of surfaces into the analysis.

3.1 Selection of the Robin parameter

For two subdomains and any Schwarz iteration $k \geqslant 1$, the equation in $\Omega_\varepsilon^\pm$ reads, for any $t_2 > t_1 \geqslant 0$,

$$\left\{ \begin{array}{lcl} P\phi^{\pm,(k)} & = & 0, \text{ on } \Omega_\varepsilon^\pm \times (t_1,t_2), \\ \mathcal{T}_\pm \phi^{\pm,(k)} & = & \mathcal{T}_\pm \phi^{\mp,(k-1)}, \text{ on } \Gamma_\varepsilon^\pm \times (t_1,t_2), \\ \phi^{\pm,(k)}(\cdot,0) & = & \phi_0 \text{ on } \Omega_\varepsilon^\pm. \end{array} \right. \tag{3.1}$$

The notation $\phi^{\pm,(k)}$ stands for the solution $\phi^\pm$ in $\Omega_\varepsilon^\pm \times (t_1,t_2)$ at Schwarz iteration $k \geqslant 0$. Initially $\phi^{\pm,(0)}$ are two given functions defined in $\Omega_\varepsilon^\pm$. For the transmission boundary conditions, the operator $\mathcal{T}_\pm = \partial_{\mathbf{n}^\pm} + \lambda \mathrm{I}$ ($\lambda \in \mathbb{R}_+^*$ or $\mathtt{i}\mathbb{R}^*$) leads to the Robin SWR DDM, and $\mathcal{T}_\pm = \partial_{\mathbf{n}^\pm} + \mathtt{i}\Lambda^\pm$, which is a nonlocal Dirichlet-to-Neumann (DtN) pseudodifferential operator, is used for the Optimal SWR imposed at any point of the interface $\Gamma_\varepsilon^\pm$ with normal vector $\mathbf{n}^\pm$. The general approach requires the preliminary construction of the symbol of $\Lambda^\pm$ by using a well-established strategy [6], in the form of an asymptotic expansion in inhomogeneous elementary symbols. In order to concretely illustrate the idea, we consider an explicit situation: the *two-dimensional* Schrödinger equation in imaginary-time. In real-time, we have

$$\left\{ \begin{array}{lcll} \mathtt{i}\partial_t \phi + \triangle \phi - V(x,y)\phi & = & 0, & (x,y) \in \mathbb{R}^2, t > 0, \\ \phi(x,y,0) & = & \phi_0, & (x,y) \in \mathbb{R}^2, \end{array} \right. \tag{3.2}$$

with $\phi_0 \in L^2(\mathbb{R}^2)$. We will also consider the cubic Schrödinger operator, where $P := \mathtt{i}\partial_t + \triangle - V(x,y) - \kappa|\phi|^2$.

We now introduce i) a fictitious domain Ω with smooth boundary Γ, and ii) a change of variables $x(r,s)$, $y(r,s)$ parameterizing Γ, where r and s are respectively the radial coordinate and the curvilinear abscissa. We then rewrite (3.2) in generalized coordinates (r,s), i.e. (real-time)

$$\left\{ \begin{array}{l} \mathtt{i}\partial_t \phi + \partial_r^2 \phi + \dfrac{1}{r}\partial_r \phi + \dfrac{1}{r^2}\partial_s^2 \phi - V_r(r,s)\phi = 0, \qquad (r,s) \in \mathbb{R}_+ \times \mathbb{R}_+, t > 0, \\ \phi(r,s,0) = \phi_0\big(x(r,s), y(r,s)\big), \qquad (r,s) \in \mathbb{R}_+ \times \mathbb{R}. \end{array} \right.$$

We denote by P_r the Schrödinger operator written in (r,s)-coordinates. We limit the analysis to two domains with smooth boundary, and defined as follows: $\mathbf{0} \in \Omega_\varepsilon^+$ and $\Omega_\varepsilon^- \cup \Omega_\varepsilon^+ = \mathbb{R}^2$. We also assume that $\Gamma_\varepsilon^+ := \partial\Omega_\varepsilon^+$ and $\Gamma_\varepsilon^- := \partial\Omega_\varepsilon^-$ are parallel at distance $\varepsilon > 0$. Let us denote by $\kappa_\varepsilon^\pm(s)$ the local curvature at $\Gamma_\varepsilon^\pm$. As in [2], we introduce the scaling factor $h_\varepsilon^\pm(r,s) = 1 \mp r\kappa_\varepsilon^\pm(s)$ and we define by $\Gamma_{\varepsilon,r}^\pm$ the parallel surface to $\Gamma_\varepsilon^\pm$ at distance $r \in [0,\varepsilon/2]$. The curvature of $\Gamma_{\varepsilon,r}^+$ is given by $\kappa_{\varepsilon,r}^+(r,s) = (h_\varepsilon^+(r,s))^{-1}\kappa_\varepsilon^+(s)$. Similarly, $\kappa_{\varepsilon,r}^-(r,s) = -(1+(\varepsilon-2r)\kappa_{\varepsilon,r}^+)^{-1}\kappa_{\varepsilon,r}^+(r,s)$ since the distance between $\Gamma_{\varepsilon,r}^+$ and $\Gamma_{\varepsilon,r}^-$ is equal to $\varepsilon - 2r$. Finally, we denote by s_ε the length of Γ_ε^+, that is $s_\varepsilon = \int_{\Gamma_\varepsilon^+} ds$, so that the curvilinear abscissa varies between 0 and s_ε. To simplify the notations, we define $\kappa_0(s)$ as the curvature at $\Gamma_{\varepsilon=0}^+$, and h_0 as the scaling factor $h_0(r,s) = 1 + r\kappa_0(s)$. We also have

$$\kappa_\varepsilon^\pm(s) = \pm h_0\big(\pm\varepsilon/2, s\big)^{-1}\kappa_0(s), \qquad \kappa_{\varepsilon,r}^\pm(s) = \pm h_0\big(\pm(\varepsilon/2 - r), s\big)^{-1}\kappa_0(s) \tag{3.3}$$

and

$$h_\varepsilon^\pm(r,s) = h_0\big(\pm(\varepsilon/2 - r), s\big) = 1 \pm (\varepsilon/2 - r)\kappa_0(s). \tag{3.4}$$

In (r,s)-local coordinates *at the subdomain interface*, the Schrödinger operator formally reads in *imaginary-time*

$$P_r := -\partial_t + \partial_r^2 + \kappa\partial_r + h^{-1}\partial_s\big(h^{-1}\partial_s\big) - V_r(r,s). \tag{3.5}$$

In the definition of the operator P_r, the notations $\kappa(r,s)$ and $h(r,s)$ stand for $\kappa_{\varepsilon,r}^{\pm}(s)$ and $h_\varepsilon^{\pm}(r,s)$, respectively, and have to be specified depending on the considered subdomain and framework. At the interfaces, the operator P_r can be formally factorized as follows (see [6]).

Proposition 3.1. The operators P_r satisfies the following Nirenberg-like factorization

$$P_r = \big(\partial_r + \mathtt{i}\Lambda_r^+(r,s,t,\partial_s,\partial_t)\big)\big(\partial_r + \mathtt{i}\Lambda_r^-(r,s,t,\partial_s,\partial_t)\big) + \mathcal{R},$$

where $\mathcal{R}\in OPS^{-\infty}$ is a smoothing operator. The operators $\Lambda_r^{\pm}$ are pseudodifferential operators of order 1 (in time). Furthermore, their total symbols $\lambda_r^{\pm} := \sigma(\Lambda_r^{\pm})$ can be expanded as

$$\lambda_r^{\pm} \sim \sum_{j=0}^{+\infty} \lambda_{r,1-j}^{\pm}, \tag{3.6}$$

where $\lambda_{r,1-j}^{\pm}$ are symbols corresponding to operators of order $1-j$. To simplify the notations, we omit here and hereafter the index r in the latter symbols (i.e. $\lambda_{1-j}^{\pm}$ stands for $\lambda_{r,1-j}^{\pm}$).

We refer to [5] for the proof of this proposition in real-time, and where a detailed construction of $\Lambda_r^{\pm}$ is iteratively established. In imaginary-time, the proof is basically identical by replacing τ by $\mathtt{i}\tau$. Let us remark that the definition of the operator $\Lambda_r^{\pm}$ is subdomain-dependent since it involves κ and h. Practically, the construction of $\Lambda_r^{\pm}$ is obtained through the computation of a finite number of elementary inhomogeneous symbols. For instance, one gets the following proposition, deduced from [5].

Proposition 3.2. Let us fix the principal symbol to

$$\lambda_1^+ = -\sqrt{-\mathtt{i}\tau - h^{-2}\xi^2 - V_r}. \tag{3.7}$$

Then, the next symbol is given by

$$\begin{aligned}\lambda_0^+ = -\frac{\mathtt{i}}{2}\kappa + \frac{\mathtt{i}}{4}\frac{(\partial_r h^{-2})\xi^2}{-\mathtt{i}\tau - h^{-2}\xi^2 + \mathtt{i}h^{-1}(\partial_s h^{-1})\xi - V_r} \\ -\frac{\mathtt{i}}{4}\frac{h^{-2}(\partial_s h^{-2})\xi^3}{\sqrt{-\mathtt{i}\tau - h^{-2}\xi^2 + \mathtt{i}h^{-1}(\partial_s h^{-1})\xi - V_r}^3}.\end{aligned} \tag{3.8}$$

Any higher order elementary operator can also be constructed. In this formalism, one gets in each subdomain

$$\lambda_r^- = -\lambda_r^+ - \mathtt{i}\kappa.$$

From (3.3) on $\Gamma_{\varepsilon,r}^{\pm}$, we have at $r=0$

$$\kappa(0,s) = \pm\big(1 \pm \varepsilon\kappa_0(s)/2\big)^{-1}\kappa_0(s), \qquad h(0,s) = 1 \pm \varepsilon\kappa_0(s)/2. \tag{3.9}$$

Unlike, the one-dimensional case, we can no more directly approximate the transparent operator by a constant, because of the dependence of $\lambda^{\pm}$ in ξ. We first need to implement an inverse

Fourier transform in ξ, denoted by $\mathcal{F}_{\xi}^{-1}\big(\lambda^{\pm}(\tau,\cdot)\big)$, before evaluating it at the subdomain interface(s). This will provide an approximation of $\Lambda^{\pm}$ if we fix τ in the asymptotic regime. The computations are long and painful but is done only once, and we refer to [6] for the details. The analytical expression of approximate values of these quantities is presented in [6] avoiding numerical FFTs, which is necessary for realistic problems. However, in 2d, we can simply obtain numerically an expression by using one-dimensional FFTs, then providing an optimized value of the Robin parameter.

Proposition 3.3. At $(r,s)=(r_i,s_i)$, we propose the following Robin parameters

- in imaginary-time, we take

$$\lambda^{+}_{(r_i,s_i)} = -\mathcal{F}_{\xi}^{-1}\big(\sqrt{-\mathtt{i}\tau_{\text{num.}}-h^{-2}\xi^2-V_r}\big)(r_i,s_i),$$

- and, in real-time, we consider

$$\lambda^{+}_{(r_i,s_i)} \quad = \quad -\mathcal{F}_{\xi}^{-1}\big(\sqrt{-\tau_{\text{num.}}-h^{-2}\xi^2-V_r}\big)\big)(r_i,s_i).$$

Moreover, in both cases, we have

$$\lambda^{-}_{(r_i,s_i)} \quad = \quad -\lambda^{+}_{(r_i,s_i)}-\mathtt{i}\kappa(s_i).$$

In practice, it is possible to get simple approximations to $\lambda^{\pm}_{(r_i,s_i)}$ for large values of $|\tau|$, involving the local curvature. In imaginary-time, up to $O(\tau^{-1})$, and assuming that $\xi^2/\tau^{1/2}$ is small enough, we obtain

$$\lambda^{+}_{r_i,s_i} \approx -\sqrt{-\mathtt{i}\tau}-\frac{\mathtt{i}}{2r_i}+\frac{V_r(r_i,s_i)}{2\sqrt{-\mathtt{i}\tau}}-\frac{\partial_{\mathbf{n}}V_r(r_i,s_i)}{4\tau}-\frac{1}{8r_i^2\sqrt{-\mathtt{i}\tau}}-\frac{1}{8r_i^3\tau}. \tag{3.10}$$

In the nonlinear case, a natural choice consists in replacing V_r by $V_r+\kappa|\phi_s(r_i,s_i)|^2$ in (3.10), where ϕ_s is an (approximate) eigenstate. However, as already explained above the contribution of the nonlinear term is *a priori* useless, except if there is no overlap.

3.2 Numerical experiments

We consider the computation on two-domains with the Robin-SWR method of the ground state by using the imaginary-time method for the following two-dimensional nonlinear cubic Schrödinger equation

$$\mathtt{i}\phi_t = -\frac{1}{2}\Delta\phi+V(x,y)\phi+\kappa|\phi|^2\phi,$$

where $\Delta=\partial_x^2+\partial_y^2$. We take $\kappa=50$ and the potential is the harmonic oscillator potential plus a potential of a stirrer corresponding to a far-blue detuned Gaussian laser beam [10] (see Fig. 10)

$$V(x,y)=25(x^2+y^2)+4e^{-((x-1)^2+y^2)}. \tag{3.11}$$

In the numerical experiment, we take the initial guess in each Schwarz iteration as

$$\phi_0(x,y)=\frac{1}{\sqrt{\pi}}e^{-(x^2+y^2)/2}. \tag{3.12}$$

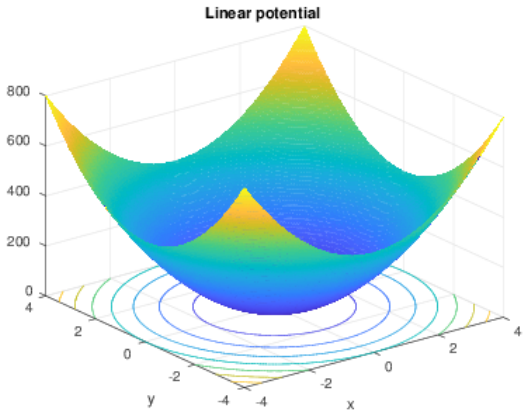

Figure 10: Two-dimensional linear potential.

The parameters of the equation and the initial guess are those of [10]. The equation is rewritten and discretized in polar coordinates (r,s) (3.3), and the global domain is the disc $\Omega_{R_1=4} = \{(r,s) \in (0,4) \times [0,2\pi)\}$. A standard semi-implicit Euler finite-difference scheme [10] is used to approximate the equation. The total number of mesh points in the r-direction is $50+50-2=96$, and 25 points are used in the s-direction. Hence, the mesh step size in the r-direction is $\Delta r = 4/(99+0.5)$ and in the s-direction $\Delta s = 2\pi/25$. The coefficient 0.5 in the denominator of Δr is introduced to circumvent the singularity issue at the origin, i.e. $1/r$. The interior and exterior domains $\Omega^{\pm}_{R_0,\varepsilon}$ have then 50 mesh points in the r-direction and where $R_0 = (50-2)\Delta r = 1.99$ denotes the radius of the interior circular subdomain. The overlapping region is a circular ring with 2 mesh points in the r-direction. Both $\Omega^{+}_{R_0,\varepsilon}$ and $\Omega^{-}_{R_0,\varepsilon}$ are then "cut" into 25 elementary segments in the s-direction. In the numerical test, we take $\Delta t = 2.5 \times 10^{-3}$ and set $\varepsilon_{\Delta r} = 2\Delta r \approx 0.08$. We compare on Fig. 11 the rate of convergence of the Robin-SWR method for different values of λ: 1, 5, 7.5, 15, 50 and 100, and an "optimized" $\lambda^{+}_{\text{Opt.}}$, corresponding to

$$\lambda^{+}_{\text{Opt.}} = -\sqrt{-\mathtt{i}/\Delta t - V_r(\text{interface}) - \kappa|\phi(t,\text{interface})|^2}.$$

The residual errors (11) are plotted with respect to the Schwarz iteration k, then showing clearly a faster convergence for $\lambda^{\pm}_{\text{Opt.}}$ compared to other choices.

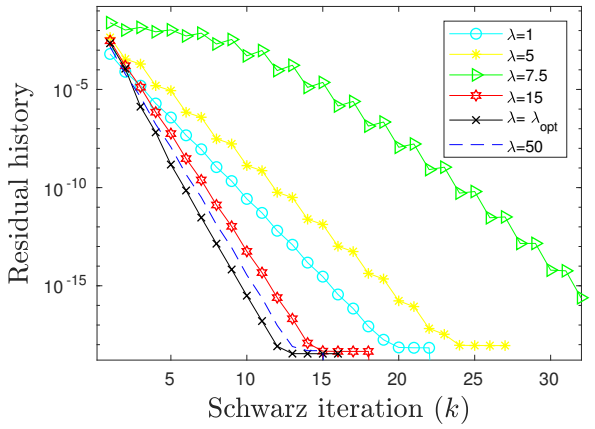

Figure 11: Comparison of SWR method convergence for different values of λ.

4 Conclusion

Thanks to an analytical approximation of the symbol of the transmission operators, it is possible to optimize the Robin parameters within the OSWR algorithms. The space- and time-dependent Robin parameter is locally selected thanks to an approximation of the transparent operator at the subdomain interfaces. The simple idea was tested and validated on the Schrödinger equation in real- and imaginary-time for one- and two-dimensional problems. The application of this idea to realistic problems in quantum chemistry is currently in progress.

Acknowledgments. X. Antoine was partially supported by the French National Research Agency project NABUCO, grant ANR-17-CE40-0025. E. Lorin received support from NSERC through the Discovery Grant program.

References

[1] X. Antoine, A. Arnold, C. Besse, M. Ehrhardt, and A. Schädle. A review of transparent and artificial boundary conditions techniques for linear and nonlinear Schrödinger equations. *Commun. Comput. Phys.*, 4(4):729–796, 2008.

[2] X. Antoine and H. Barucq. Microlocal diagonalization of strictly hyperbolic pseudodifferential systems and application to the design of radiation conditions in electromagnetism. *SIAM J. Appl. Math.*, 61(6):1877–1905 (electronic), 2001.

[3] X. Antoine and C. Besse. Construction, structure and asymptotic approximations of a microdifferential transparent boundary condition for the linear Schrödinger equation. *J. Math. Pures Appl. (9)*, 80(7):701–738, 2001.

[4] X. Antoine, C. Besse, and S. Descombes. Artificial boundary conditions for one-dimensional cubic nonlinear Schrödinger equations. *SIAM J. Numer. Anal.*, 43(6):2272–2293 (electronic), 2006.

[5] X. Antoine, C. Besse, and P. Klein. Absorbing boundary conditions for the two-dimensional Schrödinger equation with an exterior potential. Part I: Construction and *a priori* estimates. *Math. Models Methods Appl. Sci.*, 22(10):1250026, 38, 2012.

[6] X. Antoine, F. Hou, and E. Lorin. Asymptotic estimates of the convergence of classical Schwarz waveform relaxation domain decomposition methods for two-dimensional stationary quantum waves. *ESAIM: M2AN*, To appear, DOI: https://doi.org/10.1051/m2an/2017048, 2018.

[7] X. Antoine and E. Lorin. An analysis of Schwarz waveform relaxation domain decomposition methods for the imaginary-time linear Schrödinger and Gross-Pitaevskii equations. *Numer. Math.*, 137(4):923–958, 2017.

[8] X. Antoine and E. Lorin. Asymptotic convergence rates of Schwarz waveform relaxation algorithms for Schrödinger equations with an arbitrary number of subdomains. *Multiscale in Science and Engineering*, 2018.

[9] X. Antoine, E. Lorin, and A. Bandrauk. Domain decomposition method and high-order absorbing boundary conditions for the numerical simulation of the time-dependent Schrödinger equation with ionization and recombination by intense electric field. *J. of Sci. Comput.*, 64(3):620–646, 2015.

[10] W. Bao and Q. Du. Computing the ground state solution of Bose-Einstein condensates by a normalized gradient flow. *SIAM J. Sci. Comput.*, 25(5):1674–1697, 2004.

[11] C. Besse and F. Xing. Schwarz waveform relaxation method for one dimensional Schrödinger equation with general potential. *Numer. Algo.*, pages 1–34, 2016.

[12] C. Besse and F. Xing. Domain decomposition algorithms for two dimensional linear Schrödinger equation. *J. of Sc. Comput.*, 72(2):735–760, 2017.

[13] V. Dolean, P. Jolivet, and F. Nataf. *An introduction to domain decomposition methods: theory and parallel implementation*. 2015.

[14] M. Gander and L. Halpern. Optimized Schwarz waveform relaxation methods for advection-reaction diffusion problems. *SIAM J. Num. Anal.*, 45(2), 2007.

[15] M. J. Gander, F. Kwok, and B. C. Mandal. Dirichlet-Neumann and Neumann-Neumann waveform relaxation algorithms for parabolic problems. *Electron. Trans. Numer. Anal.*, 45:424–456, 2016.

[16] M.J. Gander. Overlapping Schwarz for linear and nonlinear parabolic problems. In *Proceedings of the 9th International Conference on Domain decomposition*, pages 97–104, 1996.
[17] M.J. Gander. Optimal Schwarz waveform relaxation methods for the one-dimensional wave equation. *SIAM J. Numer. Anal.*, 41:1643–1681, 2003.
[18] M.J. Gander. Optimized Schwarz methods. *SIAM J. Numer. Anal.*, 44:699–731, 2006.
[19] M.J. Gander, L. Halpern, and F. Nataf. Optimal convergence for overlapping and non-overlapping Schwarz waveform relaxation. In *Proceedings of the 11th International Conference on Domain decomposition*, pages 27–36, 1999.
[20] L. Halpern and J. Szeftel. Optimized and quasi-optimal Schwarz waveform relaxation for the one-dimensional Schrödinger equation. *Math. Models Methods Appl. Sci.*, 20(12):2167–2199, 2010.
[21] L. Nirenberg. *Lectures on linear partial differential equations*. American Mathematical Society, Providence, R.I., 1973.